RSC Advances

ROYAL SOCIETY OF CHEMISTRY

www.rsc.org/advances

COMMUNICATION

Stable Single Device Multi-Pore Electrospraying of Polymeric Microparticles *Via* Controlled Electrostatic Interactions†

Received 00th January 20xx,
Accepted 00th January 20xx

DOI: 10.1039/x0xx00000x

www.rsc.org/

Chunchen Zhang,[ab] Ming-Wei Chang,*[ab] Zeeshan Ahmad,[c] Weiwen Hu,[d] Ding Zhao,[ab] and Jing-Song Li,[a]

This work demonstrates a facile fabrication method to produce high throughput biodegradable microparticles (MPs) using a flute-like multi-pore emitter device in place of conventional single needle electrospraying capillaries. By manipulating the configuration of the emitter and the processing parameters, uniform microparticles are successfully sprayed in a single step for large-scale production. Furthermore, by manipulating individual spatial pore location various jet-bending interactions, which give rise to particle variations and irregularities, are overcome. Finally, findings correlate well with models reported by Hartman.

Polymeric MPs have well established biomedical applications, in particular serving as drug carriers for therapeutics (e.g. pulmonary, nasal, oral and transdermal delivery).[1-4] In the vast majority of cases an active pharmaceutical ingredient (API) is dispersed throughout the MP polymeric matrix which in turn is administrable *via* enteral or parenteral methods conforming to ideal release profiles to treat specific disease states and conditions.[5] In addition, polymeric MPs have shown to improve the stability and bioavailability of APIs. Encapsulation of drug within MPs can also extend the desired therapeutic effect *via* sustained delivery[6] as well as significantly reducing biotoxicity and adverse side-effects.[7]

Both synthetic and naturally occurring (biomacromolecular) polymers have been fabricated into MPs, such as chitosan, methyl cellulose, polylactic-co-glycolic acid (PLGA), Polylactic acid (PLA) and polycaprolactone (PCL).[8, 9] Amongst the synthetics, FDA approved PCL has been investigated extensively due to its excellent biocompatibility and suitability for sustained and prolonged drug delivery.[10, 11] Based on this, PCL applicability has also been explored in numerous emerging therapies such as tissue engineering and regenerative medicine.

Traditional MP fabrication methods (for polymeric systems) include polymerization, microemulsification, self-assembly, solvent evaporation and spray drying. Most of these methods require the use of surfactants or non-degradable additives which then become incorporated into the MP carrier system. Furthermore, process and manufacturing conditions can also impact API biofunctionality[12-14] by means of degrading or mechanically disrupting key features of both MP matrix material and the API.

Electrohydrodynamic atomization (EHDA) is a versatile and adaptable technique for generating monodisperse MPs with ambient parametric controls for regulated size distribution. The processing parameters include solution flow rate, applied voltage and deposition distance (orifice to collector) which can be manipulated *via* mode-mapping to achieve stable particle synthesis for a range of particle sizes.[15] Several other distinct advantages include low pressure and sheer preparation, one-pot synthesis and comparatively higher active (e.g. drug) encapsulation efficiencies when compared to existing MP preparation methods.[16] Finally, the careful manipulation and formulation of polymeric solutions to be utilised (material selection and viscoelastic properties) provides MPs with additional desirable attributes or functions.[17, 18] However, the main obstacle for industrial utility of ES generated MPs has been the scalability.

Specifically, the process generates MPs from formulated liquid (e.g. comprising API, matrix polymer and other excipients) under the influence of electrical and gravitational forces which compete with the formulated material's surface tension. The crucial stage is the enablement of a Taylor cone which leads to the most uniform MP size distribution. The process has attracted significant attention in recent years with the main focus on the preparation of nano and micron scaled fibres.[16, 19, 20] One of the key differences, however, between fibre and MP generation is the requirement of a stable cone, which is not essential for the generation of the fibrous structure type. Although these processes are highly attractive, low throughput of conventional ES methods have always been the bottleneck. With regards to process parameters, the mean diameter and quantity of generated MPs are both directly proportional to solution inflow rate. However, low flow rates are essential to produce MP drug carriers in the desired (nanometer – micrometers) range. Hence, the quantity of

[a] College of Biomedical Engineering and Instrument Science, Zhejiang University, Hangzhou, 310027, P. R. China. Email: mwchang@zju.edu.cn
[b] Zhejiang Provincial Key Laboratory of Cardio-Cerebral Vascular Detection Technology and Medicinal Effectiveness Appraisal , Hangzhou, 310027,P. R. China.
[c] Leicester School of Pharmacy, De Montfort, University, The Gateway, Leicester, LE1 9BH, UK.
[d] College of Electrical Engineering, Zhejiang University, Hangzhou, 310027, P. R. China.
† Electronic Supplementary Information (ESI) available: Experimental procedures, characterization methods. See DOI: 10.1039/x0xx00000x

generated particles becomes limited, restricting its large-scale potential in many timely biomedical and industrial applications.

Numerous devices have been developed to address this issue, with most approaches investigating microelectromechanical ES systems (MEMS). Here, high precision tools are utilized but come with amplified costs.[21-23] Lhernould *et al.* have also pointed out that even on hydrophobic surfaces (such as those found within MEMS); complicated multiple-source cone-jet generation is not stable. Furthermore, the meniscus on the apex of the nozzle may overflow and spread onto the surrounding surface, therefore resulting in MPs possessing broader diameter size distributions.[24] Also, as there are no grooves or threads separating individual ES orifices, liquid flowing out from these adjacent pores will favour spreading across the flat surface; converging into a single unstable micron stream. This also impacts on MP diameter (including uniformity) and morphology.

To address these challenges, a cost-effective flute-like multi-pore ES emitter was designed, manufactured and utilised as shown in Fig. 1. For optimization and stable uniform MP generation; polymer solution concentration, orifice properties (number, distance and size) and conventional ES processing parameters were investigated. Modeling ES behavior from the multi-pore emitter device was constructed using COMSOL Multiphysics *via* the finite element method.

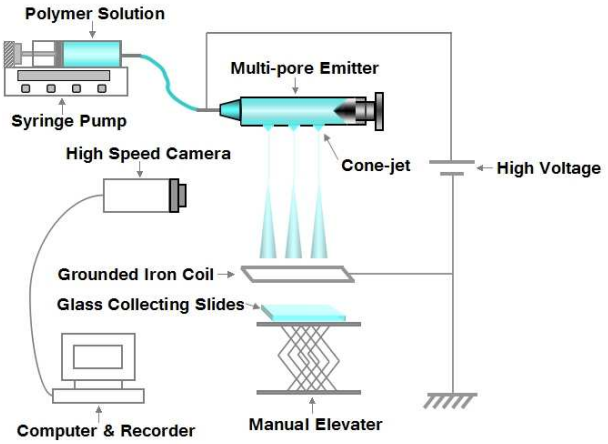

Fig. 1 Schematic illustration of the experimental setup.

For conventional (single-needle/orifice) ES processes, the polymer solution concentration is a crucial parameter to generate a stable jet and fabricate spherical solid MPs. Optical micrographs of PCL MPs prepared through the novel ES device using different polymer solution concentrations (comprising dichloromethane (DCM) and PCL) are shown in S1(a)-(f). The results indicate that lower concentrations (e.g. ≤1 wt. %) yield flat PCL particulate debris exhibiting irregular micron pores. At higher concentrations (3 wt. %), oblate particles are generated. This is attributed to increased polymeric chain entanglement thus trending towards solid spherical MP formation. Increasing this concentration further from 5 wt. % to 12 wt. %, clearly demonstrates an increase in more spherical and less random particulate morphologies. When a 9 wt. % polymer concentration is used near mono-disperse solid spherical particles are generated. Exceeding a polymeric concentration of 12 wt. %, results in fine beaded fibers which arise due to high intermolecular entanglements and rapid evaporation of the reduced solvent content.[25] In this regard the DCM solution containing 9 wt. % PCL was selected to further investigate other aspects of the flute-like multi-pore ES emitter.

Inter-orifice (pore) distance and resulting fluid/jet behaviour from two adjacent pores is also paramount for the generation of stable Taylor cones, and subsequently for the mass production of uniform MPs. When using the novel device the voltage required to enable stable cone-jet formation increased as the inter-pore interval decreased. In Figs. 2(a) and 2(b), two multi-pore ES emitters with pore intervals of 1.2 mm and 2.4 mm were subjected to the same applied voltage (18 kV) and solution flow rate (10 ml/h). Visualization of cone-jet and jet-bending dynamics were captured using a high-speed camera. As shown in Fig. 2(a), when the pore interval is relatively small (≤ 1.2 mm), jets formed from adjacent orifices were mutually exclusive and displayed similar angles of displacement relative to the central jet. If the inter-pore distance is reduced significantly, fluid flow from adjacent orifices exhibit co-flow behavior leading to repulsion between adjacent jets preventing the formation of a stable ES mode. The angle (θ) between jets (adjacent and central) is over 14° as shown by the dotted yellow lines in Fig 2a. The peripheral jets are repelled and bend outward due to columbic interactions applied by the presence of neighboring jets.[26] In this case, stable jetting is not achievable. Even if these flows do remain stable temporarily, resulting MP uniformity is not guaranteed. This is because MPs generated from the central upright jet have a shorter route compared to those from inclined jets before deposition onto the horizontal substrate. When the inter-pore interval increases (≥ 2.4 mm), the repulsive forces become weaker and stable quasi-parallel cone-jets are readily formed as shown in Fig. 2(b). In this instance near monodisperse PCL particles can be generated.

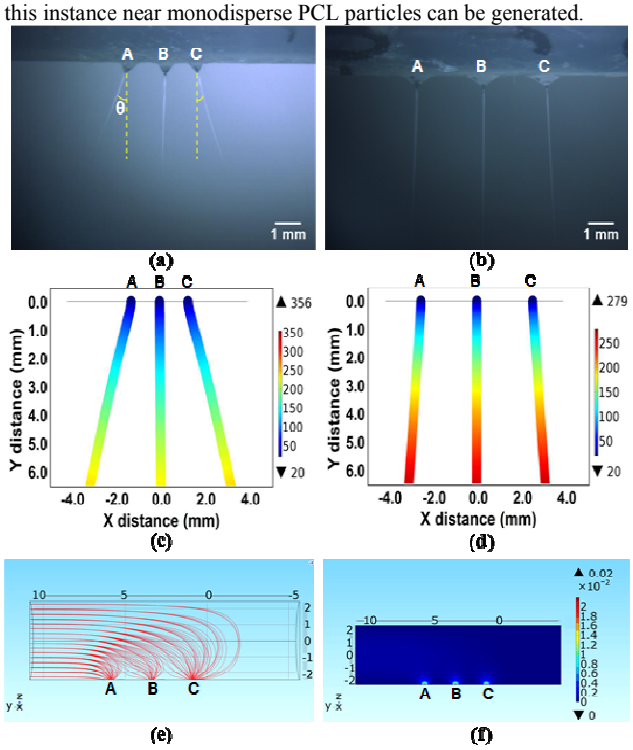

Fig. 2 Jet bending via multi-pore ES emitters with pore intervals of (a) 1.2 mm, (b) 2.4 mm. (c) and (d) are jet bending simulations (modeling) when the pore interval is 1.2 mm and 2.4 mm, respectively. The color of the bar indicates the velocity of charged particles/droplets. The unit of the indicator strip is m/s. (e) is the simulation results of the distribution of the flow field in the flute-like ES emitter when the solution is infused into the emitter from the left side, the curves indicate the trajectory of the solution. (f) The distribution of the velocity magnitude inside the flute-like emitter, the unit of the indicator strip is m/s. The units of the *xyz* three-dimensional coordinates of (e) and (f) are both in mm.

Fig. 2(c) and Fig. 2(d) are the predicted results (simulation) of jet bending phenomena during the ES process *via* a tri-pore flute-like emitter subjected to the same applied voltage (18 kV) with inter-pore intervals set at 1.2 mm and 2.4 mm, respectively. Simulation and experimental findings are consistent. Fig. 2(c) indicates that adjacent jets tend to repel each other and form a clearly evident displacement angle between them which can lead to the instability of the generated jets and the subsequent reduction in monodisperse MPs. Fig. 2(d) shows that theoretically jet-bending phenomena can be effectively suppressed when the pore interval is increased to (and beyond) a critical value (e.g. $\geq$ 2.4 mm).

Fig. 2(e) and Fig. 2(f) are simulations of flow field distribution and velocity magnitude within the flute-like ES emitter. The simulation also takes into account solution infusion rate (10 ml/h) and direction (left to right) within the ES emitter with no electric field applied. The configuration and dimensions of the simulated multi-pore emitter model were identical to those found on the device. Fig. 2(e) illustrates predictive fluid flow in the tri-pore emitter (pores: A, B, and C) where there is a tendency of the medium to be distributed at the base of the emitter. Fig. 2(f) indicates high velocity magnitude near the pores which is almost identical for all orifices (ESI†) ensuring similar flow rates and thus resulting in uniform particle size regardless of orifice origin. Furthermore, the magnitude of velocity spatially within the device is typically close to zero which ensures the multi-pore system remains at a quasi-stable state during the ES process. When comparing the multi-pore emitter to single pore/nozzle ES devices, several advantages are evident. Firstly, the production rate is appreciably increased due to greater ES capacity, converting polymeric solutions into solid MPs. Secondly, several processes utilize downstream applications (additional cost and time) to achieve the desired MP size (e.g. centrifugation). By optimizing the multi-pore processing system the MP size range can be controlled. Thirdly, using a pore system, when compared to a nozzle system, overcomes issues related to current discharge which is a common safety concern with lab based ES systems. Finally, while much lab based research has demonstrated potential proof-of-concept applications of ES generated MPs, the multi-pore developmental route provides an efficient approach to engineer a desired number of pores within a device (correlating with required MP output), which needs to be optimized for electric-field distribution and jet/spray charge interaction. However, the multi-pore emitter is still prone to other existing ES limitations as uniform particles can only be achieved under stable cone-jets. In addition solvent selection is crucial, which needs to be based on the desired end application (e.g. drug used for MP based drug delivery) requiring pre-synthesis evaluation.

Fig. 3(a) shows the effect of solution flow rate on mean MP diameter which increased from 18.5 µm at 9 ml/h to 22.5 µm at 10.5 ml/h. Furthermore, Fig. 3(b) shows the mean size of the MPs is approximately proportional to the square root of the average flow rate of each orifice, which is in good agreement with the relationship reported by Hartman[27, 28] as shown in Eq. (3), derived by Eqs. (1) and (2). The mean diameter of the MPs increases with the solution flow rate of each ES source. Herein, d stands for the diameter of the droplet (m), Q is the solution flow rate (m^3s^{-1}), ρ stands for the density of the solution, and ε_0 stands for the permittivity of vacuum, I stands for the current, γ is the surface tension of the solution in ambient air, c is a constant, and K is the conductivity of the solution. The increase in average MP size can be attributed to more solute being ejected from multiple-pores (compared to a single pore) within same amount of time. When the flow rate is over 10.5 ml/h, solvent evaporation within ES structures is not achievable before reaching the collecting substrate. Hence, many oblate particles are formed along with the spherical particles, and a broader MP size distribution is observed.

$$d = c\left(\frac{\rho\varepsilon_0 Q^4}{I^2}\right)^{1/6} \quad \text{(Eq. 1)}$$

$$I \propto (\gamma K Q)^{1/2} \quad \text{(Eq. 2)}$$

$$d \propto Q^{1/2} \quad \text{(Eq. 3)}$$

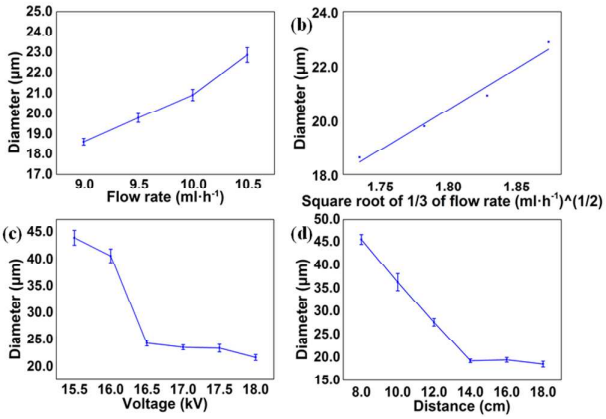

Fig. 3(a) Effects of solution flow rate on mean particle size. (b) Linear fitting of the particle size and the square root of 1/3 of the total flow rate. (c) Effects of applied voltage on particle size. (d) Effects of emitter to collector distance on particle size.

Fig. 3(c) highlights the effect of applied voltage on the mean MP diameter. A reduction in mean MP particle diameter is observed when the applied voltage was increased (~43 µm at 15.5 kV to ~21 µm at 18 kV). The steepest change was observed when the applied voltage was increased from 15.5 kV to 16.5 kV. However, incremental changes to the MP diameter were observed between an applied voltage range of 16.5-18 kV. Fig. 3(d) shows the effect of the collecting distance on the mean MP diameter which decreased from ~45 µm at 8 cm to ~17 µm at 18 cm. The mean diameter of MPs decreased significantly when the collecting distance increased from 8 to 14 cm. Over this deposition range a variation of solvent

evaporation (DCM) from generated MP droplets is expressed as changes to the solidifying MPs. A deposition distance of 14 cm appears to be the minimum distance at which the vast majority of solvent evaporates from the ejected droplets, which ultimately yields solid spherical MPs. Therefore, when the collecting distance exceeds this value (~14 cm), no further significant solvent evaporation or droplet drying (including shrinkage) is achievable.

Fig. 4 shows optical (a-d) and SEM (e-h) images of MPs generated at flow rates of 9, 9.5, 10, 10.5 ml/h, respectively. Near monodisperse solid spherical particles are observed suggesting that the new ES emitter has potential to produce uniform polymeric particles as efficiently as single-needle systems, but with greater output. The insets are high magnification micrographs of single MPs.

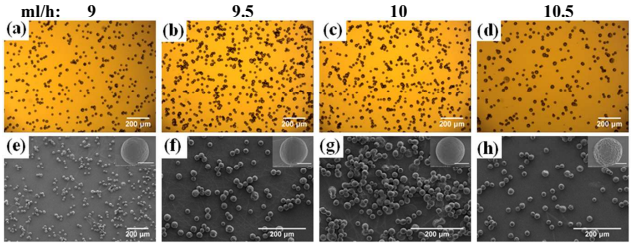

Fig. 4 Optical and SEM images of the particles generated by a multi-pore emitter at flow rate of (a) and (e) 9 ml/h, (b) and (f) 9.5 ml/h, (c) and (g) 10 ml/h, (d) and (h) 10.5 ml/h. The scale bar of the insets of (e)-(h) stands for 10 µm.

The effect of the number of orifices (or pores) on stable jetting was also investigated. Stable jetting modes using flute based; single-pore and tri-pore ES emitters (at a flow rate of 10 ml/h) are shown in Fig. 5(a) and Fig. 5(b), respectively. The tri-pore emitter can form smaller cone-jets and thinner electrojets at the same flow rate compared with the single-pore emitter, which also enables the precondition for the generation of near uniform particles in large quantities. However, the stable jetting region for PCL MP generation using single- and tri-pore emitters is demonstrated in Fig. 5(c) and Fig. 5(d), respectively. The stable jetting region of the tri-pore emitter is significantly reduced when compared to that of the single-pore version. For instance, the jetting stability zone of the applied voltage for a single-pore emitter is ~two times greater than that for the tri-pore version at fixed flow rate of 10.5 ml/h (12 kV~16 kV for a single-pore but 11 kV~13 kV for tri-pore). This is due to repulsion between adjacent jets within the tri-pore emitter when high voltage is applied. This indicates that the stable jetting region is relatively reduced when a multi-pore emitter is utilized for this up-scaled ES process. Hence, finding the optimized ES parameters for a multi-pore ES emitters is relatively economical but the operating window is narrower when compared to the single-pore system. Fig. 5(e) and Fig. 5(f) are SEM images of MPs produced by single-pore and tri-pore ES at stable cone-jet modes (fixed deposition time and substrate location) which shows improved yield of MPs from the multi-pore system.

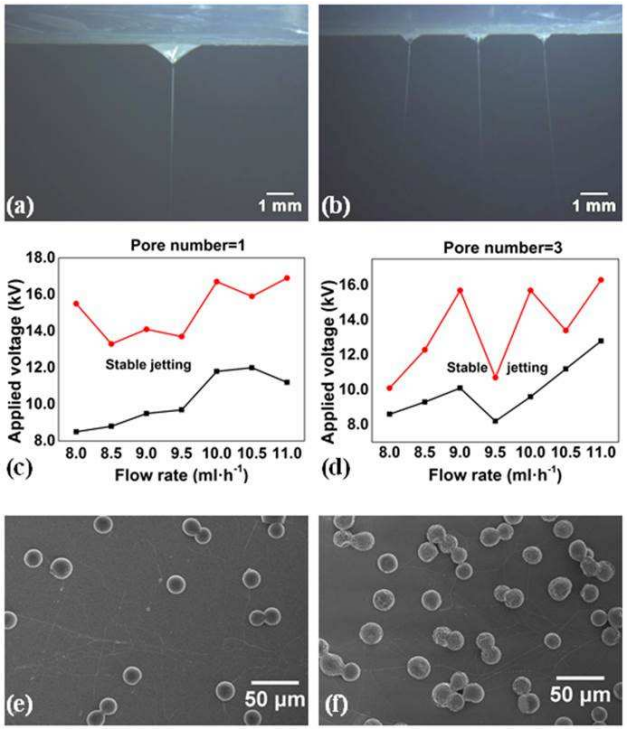

Fig. 5 (a) and (b) are images of stable jets from single-pore and tri-pore ES device, respectively. (c) and (d) are stable jetting regions (applied voltage *vs.* flow rate map) of single-pore and tri-pore processes, respectively. (e) and (f) are SEM images of generated MPs using single-pore and tri-pore systems at stable cone-jet modes, respectively.

In this article, the design and utilization of a flute-like multi-pore ES emitter was successfully demonstrated to produce monodisperse PCL particles. Simulation results of the novel ES system were in strong agreement with the experimental findings. By tailoring the processing parameters, controlled up-scaled PCL MP production is feasible. The ES emitter provides a highly valuable approach for the design and prediction of emerging active encapsulated MPs with high throughput and low cost for a wide range of therapies.

ES methods have been deployed to generate particles ranging from the nano- to micro-meter scale for various size dependent applications. In many instances the orifice or needle geometry has been maintained (fixed) and the particle size has been manipulated using media flow rate, applied voltage and deposition distance. The impact of these parameters is well documented. [16] In this regard the multi-pore system can be adjusted using these variables (based on desired application). Ding et. al., have successfully generated PCL MPs (10 to ~30µm using single needle ES for drug delivery applications;[15] similar in size to what is reported in this study. The utility of MPs for biomedical applications (e.g. drug delivery, regenerative medicine, medical device coatings) are not limited to sizes below 10 µm, which is the case for intravenous (I.V.) drug delivery. For other drug delivery routes (e.g. oral and pulmonary delivery[29]) the size range demonstrated in this study is fit for purpose and is also applicable for advanced tissue engineering where cell encapsulation using ES methods need to accommodate living biological systems (>15 µm).[30]

Although differences in MP size (based on jet-angle) seem minute, these become substantial for MP packing/loading (e.g. into a medical device or engineered scaffold which comprise layers of MPs). Here, even small size disparities impact MP ordering thus minimizing achievable loading content. In addition, for drug delivery applications, the closer the particle size distribution, the more reliable the release kinetics.

The utilization of ES to generate MPs has received significant attention within biomedical remits (e.g. drug delivery and tissue engineering). The bottleneck for these methods have largely centered on scalability and cost of device development. In this study a facile, cost-effective and scalable multi-pore emitter was developed demonstrating potential to address key issues aforementioned. Further explorations will now focus on exploiting this new approach to fabricate homogeneous, multi-functional and composite particles for drug delivery on a large-scale.

This work was financially supported by the National Nature Science Foundation of China (81301304), and the Central Universities (2013QNA5003), and the Research Fund for the Doctoral Program of Higher Education of China (20130101120170).

Notes and references

1. S. Sunoqrot, J. Bugno, D. Lantvit, J. E. Burdette and S. Hong, *Journal of Controlled Release*, 2014, **191**, 115-122.
2. T. Suzuki, A. Osumi and H. Minami, *Chemical Communications*, 2014, **50**, 9921-9924.
3. S. De Koker, R. Hoogenboom and B. G. De Geest, *Chemical Society Reviews*, 2012, **41**, 2867-2884.
4. H. Wang, F. Xu, D. Li, X. Liu, Q. Jin and J. Ji, *Polymer Chemistry*, 2013, **4**, 2004-2010.
5. B. Almería, T. M. Fahmy and A. Gomez, *Journal of Controlled Release*, 2011, **154**, 203-210.
6. B. Almería, W. Deng, T. M. Fahmy and A. Gomez, *Journal of Colloid and Interface Science*, 2010, **343**, 125-133.
7. H. K. Makadia and S. J. Siegel, *Polymers*, 2011, **3**, 1377-1397.
8. V. Lassalle and M. L. Ferreira, *Macromolecular bioscience*, 2007, **7**, 767-783.
9. S. D. Nath, S. Son, A. Sadiasa, Y. K. Min and B. T. Lee, *International journal of pharmaceutics*, 2013, **443**, 87-94.
10. V. Sinha, K. Bansal, R. Kaushik, R. Kumria and A. Trehan, *International journal of pharmaceutics*, 2004, **278**, 1-23.
11. M. A. Woodruff and D. W. Hutmacher, *Progress in Polymer Science*, 2010, **35**, 1217-1256.
12. X. D. Guo, J. P. Tan, S. H. Kim, L. J. Zhang, Y. Zhang, J. L. Hedrick, Y. Y. Yang and Y. Qian, *Biomaterials*, 2009, **30**, 6556-6563.
13. K.-R. Kim, D.-R. Kim, T. Lee, J. Y. Yhee, B.-S. Kim, I. C. Kwon and D.-R. Ahn, *Chemical Communications*, 2013, **49**, 2010-2012.
14. C. G. Gaete, N. Tsapis, L. Silva, C. Bourgaux and E. Fattal, *european journal of pharmaceutical sciences*, 2008, **34**, 12-21.
15. L. Ding, T. Lee and C.-H. Wang, *Journal of Controlled Release*, 2005, **102**, 395-413.
16. R. Sridhar, R. Lakshminarayanan, K. Madhaiyan, V. Amutha Barathi, K. H. C. Lim and S. Ramakrishna, *Chemical Society Reviews*, 2015, **44**, 790-814.
17. D. M. Correia, R. Gonçalves, C. Ribeiro, V. Sencadas, G. Botelho, J. G. Ribelles and S. Lanceros-Méndez, *RSC Advances*, 2014, **4**, 33013-33021.
18. R. Gonçalves, P. Martins, D. M. Correia, V. Sencadas, J. L. Vilas, L. M. León, G. Botelho and S. Lanceros-Méndez, *Rsc Advances*, 2015, **5**, 35852-35857.
19. Y. Wu, I. C. Liao, S. J. Kennedy, J. Du, J. Wang, K. W. Leong and R. L. Clark, *Chemical Communications*, 2010, **46**, 4743-4745.
20. N. Bock, T. R. Dargaville and M. A. Woodruff, *European Journal of Pharmaceutics and Biopharmaceutics*, 2014, **87**, 366-377.
21. S. B. Q. Tran, D. Byun, V. D. Nguyen, H. T. Yudistira, M. J. Yu, K. H. Lee and J. U. Kim, *Journal of electrostatics*, 2010, **68**, 138-144.
22. W. Deng, C. M. Waits, B. Morgan and A. Gomez, *Journal of Aerosol Science*, 2009, **40**, 907-918.
23. R. Bocanegra, D. Galán, M. Márquez, I. Loscertales and A. Barrero, *Journal of Aerosol Science*, 2005, **36**, 1387-1399.
24. M. S. Lhernould and P. Lambert, *Journal of electrostatics*, 2011, **69**, 313-319.
25. N. Bock, M. A. Woodruff, D. W. Hutmacher and T. R. Dargaville, *Polymers*, 2011, **3**, 131-149.
26. S. Theron, A. Yarin, E. Zussman and E. Kroll, *Polymer*, 2005, **46**, 2889-2899.
27. R. P. A. Hartman, D. Brunner, D. Camelot, J. Marijnissen and B. Scarlett, *Journal of Aerosol Science*, 1999, **30**, 823-849.
28. R. Hartman, D. Brunner, D. Camelot, J. Marijnissen and B. Scarlett, *Journal of Aerosol Science*, 2000, **31**, 65-95.
29. H. Kim, H. Park, J. Lee, T. H. Kim, E. S. Lee, K. T. Oh, K. C. Lee and Y. S. Youn, *Biomaterials*, 2011, **32**, 1685-1693.
30. V. L. Workman, L. B. Tezera, P. T. Elkington and S. N. Jayasinghe, *Advanced Functional Materials*, 2014, **24**, 2648-2657.

Graphical abstract:

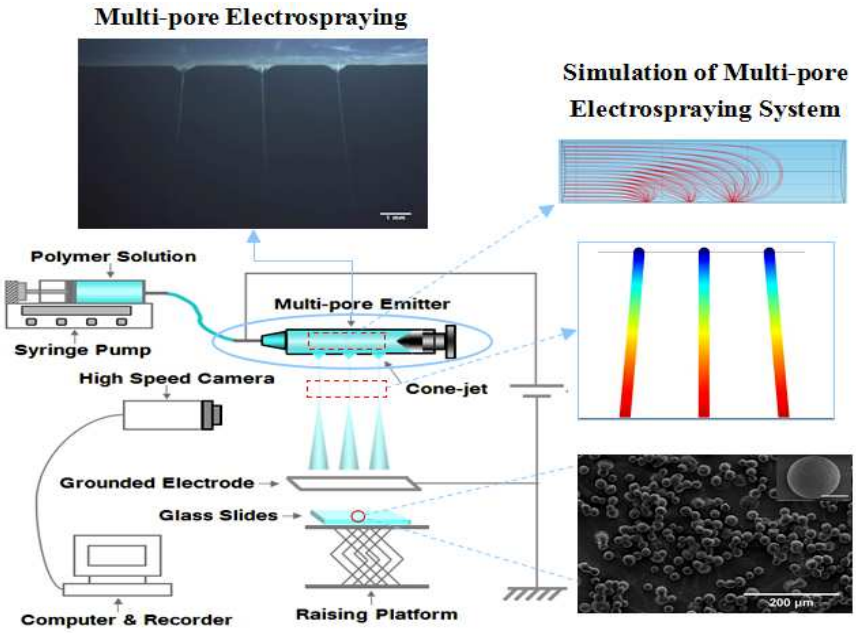

A novel flute-like multi-pore electrospray emitter was designed and manufactured to enable economical scale-up smooth spherical microparticles. The effect of processing parameters and device configuration on particle sizes is described.